3D crack network during the scratching of a polymer: comparison between experimental results and localized multigrid X-FEM

M.C Baietto Dubourg[1], J. Rannou [1], A. Gravouil[1], H. Pelletier[2], C. Gauthier[2], R. Schirrer[2]
[1]*LaMCoS CNRS UMR 5259 Villeurbanne, France;*
[2]*ICS CNRS UPR 22 Strasbourg, France*

Abstract

Attempts have been made to correlate the scratch behavior and basic material properties of polymers and a correlation has been established between the scratch damage, the bulk response and the friction coefficient. The scratch behavior of a thermoset solid polymer exhibiting brittle behavior in tension was investigated to determine how the behavior of the bulk material affects the scratch resistance. The surfaces were scratched under progressive scratch loading and an imaging system was used to record real time photographs of the in-situ contact area and scratch damage corresponding to cracking near the rear edge of the contact. The 3D crack pattern has been analyzed using fluorescence confocal laser scanning microscopy. A finite element simulation gave an estimation of the contact loading used as input data for the 3D crack network onset and development analysis based on 3D localized multigrid X-FEM techniques. The level sets functions are defined from the measured crack geometry. A set of 11 localized multigrid meshes are used to focus on the cracked and contact areas. The accurately computed stress distributions within the 3D cracked are of great interest to understand the crack network formation observed during the experiments. This combined approach opens the way for identifying and even validating 3D crack propagation modeling.

1 Introduction

Many authors have studied damage to polymeric surfaces during scratching [1], [2],[3], [4] and it has been found to take the form of open or closed cracks. The assumption generally retained to explain this cracking is the existence of tensile stress at the rear edge of the contact. The diversity of the damage nevertheless suggests that it does not occur through a single mechanism. In addition, no clear relationship has been established between the bulk response and scratch damage. The scratch behavior of solid polymers was therefore investigated to determine how the behavior of the bulk material affects the scratch resistance. To enhance the understanding and to get a more systematic predictive approach, experimental tests and a numerical approach are combined. A CR39 polymer is chosen for this comparison as it displays brittle tension behavior. An accurate experimental in-

situ and continuous monitoring of crack formation during controlled scratch loading is performed. Data essential for the numerical simulation such as sphere/plane friction coefficient, 3D surface crack shape and the distance between consecutive cracks are recorded. Complementary observations gave 3D in-depth crack shape. This 3D crack network is then modeled numerically by using a multiscale model based on a coupled local multigrid and eXtended Finite Element method within the linear fracture mechanics framework. Levels sets techniques are used to define the 3D crack shape. The paper is organized as follows. Section 2 presents the experimental device and results. Section 3 displays the numerical model. Section 4 introduces the scratching simulation and discusses the comparison between experimental and predicted results. In section 4, some concluding remarks and points for further research are given.

2. Material, experimental device and scratch analysis

2.1 Materials

The organic glass is an amorphous thermoset polymer (diethylene glycol bis(allyl carbonate)) called CR39. Its Young modulus is typically 2 GPa at 20 °C and 1 Hz. Compressive (see Fig. 1), tensile and scratch test have been performed. It is important to note that the CR39 breaks at about 1% in case of tensile test.

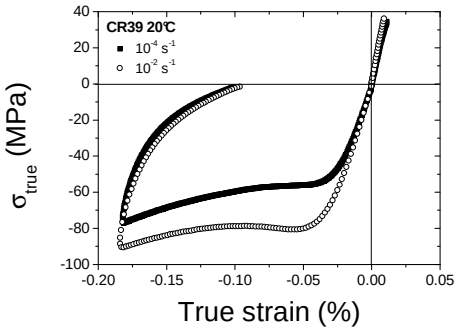

Figure 1: CR39 stress strain curves for two strain rates for compressive tests.

2.2 Experimental device

An in-situ experimental device previously developed was used to study the initiation of damage [5]. It consists of a commercial servomechanism bearing a temperature controlled transparent small box containing both the sample and the scratching tip. Control of the moving tip and recording of the normal F_n and tangential F_t loads, scratching speed V and temperature T are computer driven. A built-in microscope allows in-situ and continuous observation and measurement

of the surface wake. Scratching over a wide range of speeds (1 to 10^4 µms^{-1}) and within a temperature range covering the polymer relaxation peaks (-70 to +120 °C) are the main innovative features of the system. F_n can vary from 0.05 to 35 N. The present experiments have been performed at constant V=10^2 µms^{-1} and T=20°C. A cone-shaped diamond tip with a spherical radius R of 116 µm and an apex angle of 60° was used.

2.3 Experiments

A standard procedure was used to carry out the friction tests. After cleaning both the tip and the sample with alcohol and drying them, a preliminary test was performed to age the tip surface against the polymer counter face to get reliable and reproducible results. A single-track scratch test was then performed, consisting in applying the lowest normal load 0.1N and increasing it progressively up to 5 N to explore the whole strain sensitivity range. The normal load was then adjusted at the "critical level" corresponding to the beginning of cracking. More

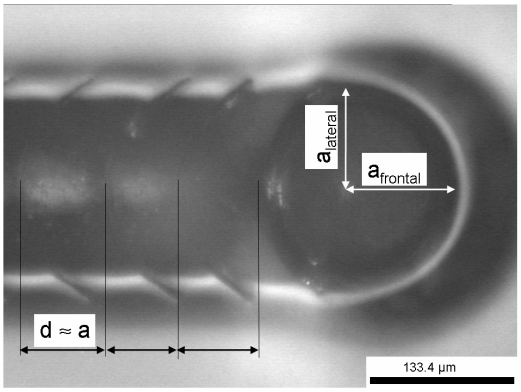

Figure 2: in-situ photograph of CR39 damage. Cracking appears near the rear edge of the contact area. a/R = 0.8

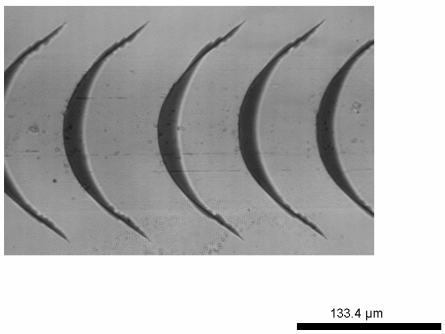

Figure 3: post mortem photograph of the surface cracking pattern. a/R=0.8

that ten scratches were achieved to ensure the test reproducibility. In-situ pictures were taken to record information on the shape of the contact area, the cracking and the groove (See Fig. 2). A series of curved periodic cracks concave to the wake are formed at the rear edge of the contact and propagate along an inclined angle up to a depth of a few tenths of micrometers for a 4.3 N normal load (See Fig. 3). d/a and mp/a ratios, distance between two consecutive cracks to contact radius ratio and maximum depth along the crack profile to contact radius ratio, are both roughly equal to 1. Immediately after initiation, the crack extremities extend and radiate out of the frontal contact area of radius a. The regular spacing of the observed crack pattern suggests that the cracks are successively nucleated according to an unloading/reloading process. The photograph evidences some

viscoelasticity and plasticity: the edges of the surface groove lie parallel but display a large self healing after 24h. Post-scratching analyses are performed using confocal laser scanning microscopy. It is an optical imaging technique that can be used to reconstruct 3D images. To reveal the fracture surface, the CR39 sample was immersed in a fluorescent solution. Figures 4 and 5 present the 3D reconstruction of the cracking pattern and the longitudinal section respectively.

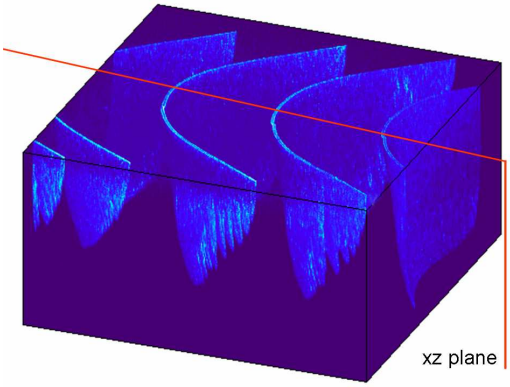

Figure 4: 3D crack pattern reconstruction: The surface fracture is roughly a part of a cylinder. a/R=0.8. d /a ≈ 1, mp/a ≈ 1.

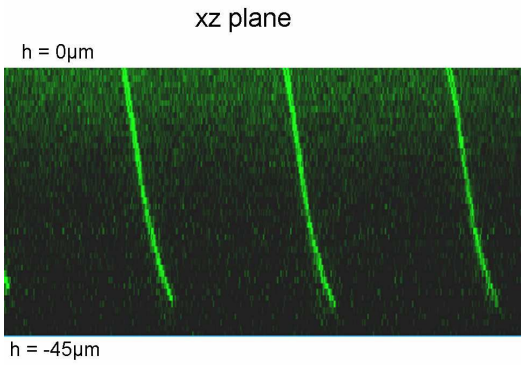

Figure 5: longitudinal section of the cracking pattern. The fractures are inclined at about 15° from the top free surface in the sliding direction. a/R=0.8

2.4 Numerical simulation of the scratching condition

A three dimensional finite element modeling based on MSC Marc Code of a spherical indenter sliding over the CR39 sample was conducted. The domain is modeled as a quarter of a cylinder as shown in Figure 6. No remeshing is performed during the simulation. The detail of the specific finite element mesh is defined in [6].

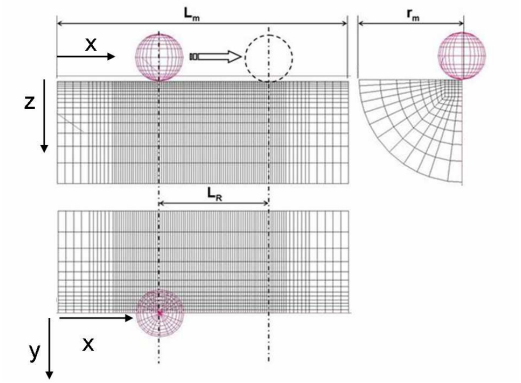

Figure 6: FE mesh of a spherical indenter sliding over the CR39 cylinder

Despite the fact that the elasticity of polymers is often non linear at a given temperature and strain rate, the elastic behavior was modeled with a linear

incremental law defined by Young's modulus E and Poisson's ratio ν, both taken to be constant and determined in a compressive test. The flow stress was described by a G'sell-Jonas law [7] and the parameters of this law were determined by an inverse method adapted to large deformations and based on interpretation of the force-penetration curves in indentation tests with two indenter shapes [8], [9].The assessed value of the friction coefficient of 0.2 [10] is here used as an input data for the simulation while *a/R* ratio is progressively increased. Figure 7 shows the contact pressure and the tangential traction distributions numerically computed. The comparison between the present finite element mean contact pressure of about 225 MPa with the 200 MPa mean contact pressure assessed from the in situ observation is good. It is well known that below the glass temperature, the mechanical properties of polymeric materials increase linearly with the logarithm of the strain rate as predicted by Eyring's law. Just as the scratch hardness was classically written as a function of the yield stress, the contact pressure may be written as a function of the yield stress with a factor c depending on the contact strain (see Eq.1):

$$p(T,\dot{\varepsilon}) / \sigma_y(T,\dot{\varepsilon}) = c(\varepsilon) \qquad (1)$$

This contact pressure to yield stress ratio called the normalized contact pressure, is time and temperature independent and depends only on the strain in the contact area [11] The major assumption made here is the decoupling of the strain dependency and the temperature and velocity dependency. As during the experiments the in-situ observation give an information of the contact pressure $p(T,\dot{\varepsilon})$ and of the cracking size for known values $(T,\dot{\varepsilon})$, it is licit to analyze the cracking mechanism without taking into account the time and temperature dependencies. The subsequent analysis of the fracture process is thus based on the linear elastic fracture mechanics.

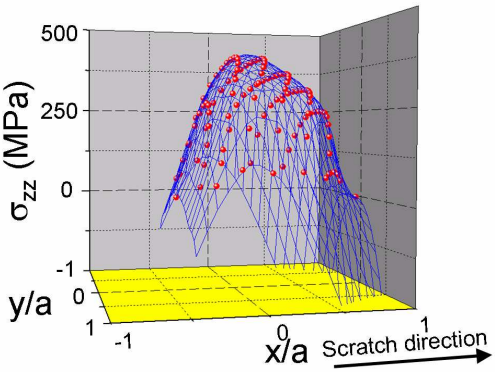

Figure 7: 3D FE pressure distribution. Peak value Po = 400 MPa

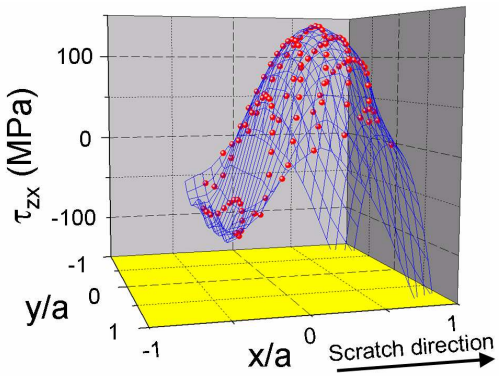

Figure 8: 3D FE traction distribution. Peak value To = 150 MPa

3 Localized MultiGrid Extended Finite Element (LMG-XFEM) formulation for linear elastic fracture mechanics

The eXtended Finite Element method (X-FEM) coupled with the level set method yields a powerful numerical tool enable to tackle complex solid mechanics problems, in particular 3D crack modeling and propagation [12], [13]. The level set formalism [15], [14] allows for a numerical accurate 3D crack geometry representation. The X-FEM enrichment functions, added to the Finite element approximation according to the partition of unity method allow (i) to model a crack whose geometry is non conform with the mesh and (ii) leads to a good approximation of the crack front singular field. These significant advantages might be insufficient with regard to industrial cracking problems in which several orders of magnitude lie between the characteristic lengths of the crack and the structure. Actually only small parts of the computational domain require a refined mesh. A multiscale approach has thus been proposed resting on the X-FEM level set combination with a local multigrid technique [16]. The outline of the approach will be presented hereafter. Then the numerical model will be used to analyze the 3D crack network formation and behavior during a polymer scratching.

3.1 LMG-X-FEM numerical model

Multigrid techniques allow solving in reasonable time and at low memory requirements large 3D problems, unattainable with solvers based on direct methods. Initially introduced by Brandt [17], they were extended to the finite element method by Parsons and Hall [18] for solid mechanic applications. The complexity, i.e. the number of operations, only grows linearly with the number of unknowns. They are based on an iterative solver combined with a sequence of nested grid levels to use the ability of iterative solver, such as conjugate gradient, to capture the high frequency part of the solution for each grid level with maximal efficiency. Specific intergrid operators (prolongation and restriction) are used to transfer primal (displacement resp. displacement corrections) and dual (nodal forces resp. residuals) quantities between the grids. In the FEM framework, these operators are build using the shape functions. The coupling with XFEM has led to several developments concerning:

- the intergrid operators: a great attention has been devoted to their construction due to the localized nature of enrichments in the crack area [19].
- a local multigrid algorithm [16] based on the Full Approximation Scheme (FAS), is used to handle localized meshes
- a specific multiscale enrichment strategy leading to an optimal multigrid convergence has been developed
- a single independent level set definition, based on a structured distinct finite difference grid. It avoids definitions of level sets for each grid level while improving the crack description accuracy. The level set discretization is possibly finer than the one of the structure, it is only localized in the area of interest and very robust schemes defined within the finite difference framework can be used for the level set operations [15].

In case of localized multiscale problems, encountered for instance with cracks in structures, it is of utmost opportunity to restrict the higher resolution meshes to small domains while the coarser ones are defined on the whole structure and related to the structure scale.

3.2 3D network tension cracks under a sliding spherical indenter

2D calculations have been performed previously to analyze the formation of a network of 3D regularly spaced curved cracks concave to the wake of the spherical indenter within polystyrene films [20]. The aim here is to investigate the 3D crack behavior and to get a first insight into the development of such crack pattern with a particular emphasis on the 3D aspects. Within the context of the present investigation, some simplified assumptions are formulated:

- The assessed friction coefficient at the indenter/CR39 interface obtained from the scratching tests is used as input data. The pressure and tangential traction distributions at the rigid tip and the CR39 sample interface obtained using the 3D finite element analysis described in §2 without accounting for the presence of the cracks, are incrementally shifted from the starting position during the sliding of the spherical indenter.
- the CR39 is assumed to behave elastically as the loading conditions selected - tip displacement velocity, temperature, normal load are such that it displays no sensitivity to the strain rate. Young's modulus, Poisson's ratio are further supposed constant and taken as E=2,1GPa and ν =0,3.
- We assume that the dominant fracture mechanism is mode I. The crack network, regularly spaced, is observed at the rear of the contact, where a tensile stress state occurs and the CR39 exhibits a brittle behavior in tension.
- The contact is not accounted for between the crack faces. The cracks undergo tensile stresses and are opened as long as the indenter is close enough.

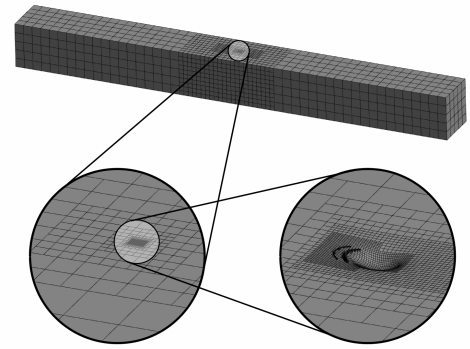

Figure 9: CR39 slab with 11 localized multigrid nested meshes. L/b=3300 is the slab length to crack length ratio

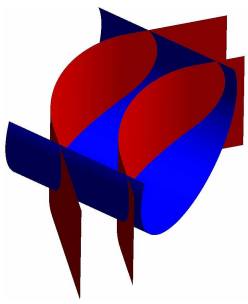

Figure 10: Crack pattern definition according to 3D signed distance functions

The respective dimensions for the CR39 sample, the crack (d/a ≈ 1, mp/a ≈1), the contact area (a) and the distributions of the pressure and tangential tractions (Po, To) are defined in order to respect the experimental characteristics. The CR39 sample is h=1mm in height, t=1mm in thickness and L=10mm in length (see Fig. 9). The contact area, is supposed to be elliptical, with semi-axes equal to 3µm and 5µm respectively. The pressure and the tangential distributions peak values are 400 and 150 MPa. The simulations have been conducted using the Elfe_3d code based on the LMG-X-FEM model. 11 hierarchical nested and localized meshes are used so that a ratio of 1024 between the coarsest and the finest grid element is achieved (see Fig. 9). The highest resolution part of the domain is located in the zone surrounding the crack but also in the loading zone neighborhood where steep gradients hold. Note that this refined zone follows the loading zone displacement. The crack surface is approximated within the level set formalism to be a 3.2µm radius cylinder. The front position is given by the intersection of this cylinder with a second 3µm radius cylinder whose axis is orthogonal to the first one and located on the sample surface (see Fig. 10). This geometry is very close to the real crack shape (see Fig. 4). These level set functions are discretized on an auxiliary 60x28x32 element mesh covering a 6µmx4µmx4µm domain

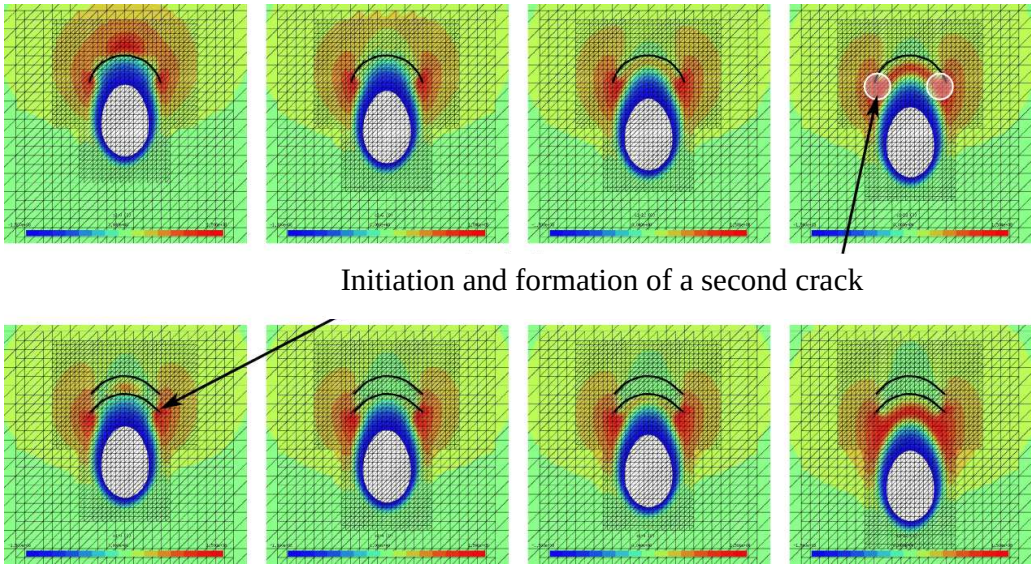

Figure 11: Surface maximum tensile principal stress σ_1 during the indenter sliding for one and then 2 cracks distanced from d. Maximum and minimum values equal to 150 and -150 MPa.

At the beginning of the simulation, a single crack is considered. The finite element pressure and tangential distributions computed in §2.4 and associated to the spherical indenter sliding are incrementally shifted from a starting position defined with respect to the crack location. The corresponding stress and strain fields within the cracked sample are computed for those different locations. The surface maximum principal stress field σ_1 thought to be responsible for mode I

tensile cracking is displayed on figure 11 for different locations. Without any crack and in case of a tangential load added to the normal one, the maximum value is classically reached at the rear of the contact zone. Here, the stresses are strongly modified. Two symmetric maxima located at the crack surface tips are observed while the crack opening unloads the contact rear. As the sliding distance is further increased and the load moves away from the crack, these tensile zones extend from both crack extremities at the surface and progressively merge at the rear edge of the contact zone in the meridian plane. Concomitantly the intensity of σ_1 increases. This suggests that the formation of new cracks will start from those two locations where the tensile stress is rebuilt up to a critical value associated with the CR39 strength. A second identical crack is then numerically superimposed according to a brittle fracture process at a distance of 3µm. The two cracks unload again the material and the stress field behaves as previously. This unloading/reloading process is responsible for the successive nucleation of the cracks and their regular spacing.

4 Conclusion

A 3D crack network during the scratching of a polymer has been continuously in-situ observed. Assessed data from the measurements have been used as input data for a 3D linear elastic numerical modeling based on the eXtended Finite Element Method coupled with localized Multigrid techniques. Based on the assumption that the crack mechanism is predominantly driven by mode I, the fracture process responsible for the crack pattern formation has been identified as a complex 3D unloading/reloading process.

Acknowledgment

The authors would like to acknowledge Dr Schröder André - ICS, for the high-resolution optical images obtained with the confocal laser scanning microscopy.

References

[1] B.J. Briscoe, E. Pelillo, S.K. Sinha, Scratch hardness and deformation maps for polycarbonate and polyethylene. Polymer Engineering and Science, 36, (1996), 2996-3005.
[2] A.C.M. Yang, T.W. Wu, Wear and friction in glassy polymers: Microscratch on blends of polystyrene and poly(2,6-dimethyl-1,4-phenylene oxide). Journal of Polymer Science Part B: Polymer Physics, 35, (1997), 1295-1309.
[3] M. Wong, A. Moyse, F. Lee, H.-J. Sue, Study of surface damage of polypropylene under progressive loading. Journal of Materials Science, 39, (2004), 3293-3308.

[4] V. Jardret, P. Morel, Viscoelastic effects on the scratch resistance of polymers: Relationship between mechanical properties and scratch properties at various temperatures. Progress in Organic Coatings, 48, (2003), 322-331.
[5] C. Gauthier, R. Schirrer, Time and temperature dependence of the scratch properties of poly(methylmethacrylate) surfaces. Journal of Materials Science, 35, (2000), 2121-2130.
[6] H. Pelletier, A.-L. Durier, C. Gauthier, R. Schirrer, Viscoelastic and elastic-plastic behaviors of amorphous polymeric surfaces during scratch. Tribology International, 41, (2008), 975-984.
[7] C. G'Sell, J.J. Jonas, Determination of the plastic behaviour of solid polymers at constant true strain rate. Journal of Materials Science, 14, (1979), 583-591.
[8] J. L. Bucaille, E. Felder, and G. Hochstetter, Experimental and three-dimensional finite element study of scratch test of polymers at large deformations. Journal of Tribology, 126, (2004), 372-379
[9] J.-L. Bucaille, C. Gauthier, E. Felder, R. Schirrer, The influence of strain hardening of polymers on the piling-up formation during scratch tests: experiments and numerical modelling. Wear 260,(2006) 803-814
[10] S. Lafaye, C. Gauthier, R. Schirrer, A surface flow line model of a scratching tip: Apparent and true local friction coefficients .Tribology International, 38, (2005), 113-127
[11] C. Gauthier, A.-L. Durier, C. Fond, R. Schirrer, Scratching of a polymer and mechanical analysis of a scratch resistance solution. Tribology International, 39 (2006), 88-98.
[12]N. Moes, J. Dolbow, T. Belytschko. A finite element method without remeshing. Int. J Numer Methods Engrg, 46 (1) (1999), 131-150
[13] T. Belytschko, T. Black, Elastic crack growth in finite element with minimal remeshing. Int. J Numer Methods Engrg, 45 (5), (1999), 601-620.
[14] A. Gravouil, N. Moes, T. Belytschko, Non planar 3D crack growth by the extended finite element and level sets- Part II : level set update. Int. J Numer Methods Engrg, 53,(2002), 2569-2586
[15] J.A. Sethian level set methods and fast marching methods. Cambridge University Press, Cambridge, 1999
[16] J. Rannou, A. Gravouil, M.-C Baietto-Dubourg. A local multigrid X-FEM strategy for 3D crack propagation Int. J Numer Methods Engrg (2008). To be published
[17] A. Brandt, Multilevel adaptive solutions to boundary-value problems, Math Comput 31 (1977) 333-390
[18] I. Parsons, J. Hall, The multigrid method in solid mechanics: Part I: algorithm description and behavior, Int. J Numer Methods Engrg 29, (1990), 719-737
[19] J. Rannou, A. Gravouil, A. Combescure. A multigrid extended finite element method for elastic crack growth simulation. Eur. J. Comput Mechanics (2007), 16 161-182
[20] A. Chateauminois, M.-C Baietto-Dubourg, C. Gauthier, R. Schirrer, In situ analysis of the fragmentation of polystyrene films within sliding contacts, Trib. Int. (2005), 38, 931-942.